Modeling deep ocean shipping noise in varying acidity conditions

Ilya A. Udovydchenkov[a] **and Timothy F. Duda**
Applied Ocean Physics and Engineering, Woods Hole Oceanographic Institution, Woods Hole, Massachusetts 02543
ilya@whoi.edu, tduda@whoi.edu

Scott C. Doney and Ivan D. Lima
Marine Chemistry and Geochemistry Department, Woods Hole Oceanographic Institution, Woods Hole, Massachusetts 02543
sdoney@whoi.edu, ilima@whoi.edu

Abstract: Possible future changes of ambient shipping noise at 0.1–1 kHz in the North Pacific caused by changing seawater chemistry conditions are analyzed with a simplified propagation model. Probable decreases of *p*H would cause meaningful reduction of the sound absorption coefficient in near-surface ocean water for these frequencies. The results show that a few decibels of increase may occur in 100 years in some very quiet areas very far from noise sources, with small effects closer to noise sources. The use of ray physics allows sound energy attenuated via volume absorption and by the seafloor to be compared.

PACS numbers: 43.30.Cq, 43.30.Es, 43.30.Nb [GD]
Date Received: February 2, 2010 **Date Accepted:** March 26, 2010

1. Introduction

It has been known for several decades that a reduction of ocean *p*H (increase of acidity) would also reduce chemical relaxation-based acoustic energy loss (Mellen and Browning, 1977; Francois and Garrison, 1982). A positive flux of carbon dioxide into the ocean has already reduced *p*H in the upper ocean. This trend has been forecast to accelerate due to fossil fuel combustion and rising atmospheric CO_2 (for example, Caldeira and Wickett, 2005; Feely *et al.*, 2009). Recent global maps of predicted changes in low-frequency sound absorption coefficient α (Ilyina *et al.*, 2010) are in agreement with other global biogeochemical studies, and show that an effect of net carbon dioxide flux into the ocean is likely to be reduction of *p*H of order 0.3–0.5 units over the next 100 years, although with markedly reduced effect in many areas at depths exceeding 1000 m. The associated effect on the volume absorption coefficient at 100–1000 Hz in affected waters will be a decrease of approximately 40%–50%.

It has been pointed out that a 40% reduction of the absorption coefficient will allow sound to travel 70% further (retaining a reference sound pressure level), all else being equal (Brewer and Hester, 2009). Thus, the absorption reduction has been conjectured to have potential effects on marine organisms sensitive to sound (Brewer and Hester, 2009; Ilyina *et al.*, 2010). However, the 70% value is true only for plane waves, which are not produced by localized sources in the ocean sound channel. Spreading loss effects for the non-plane waves found in the ocean are well known; for example, sound pressure level falls as distance squared from a point source. Here, sound pressure level (SPL) in dB equals $10\log_{10}(p^2/p_{\mathrm{ref}}^2)$, where p is sound pressure and p_{ref} is a reference pressure, conventionally 1 μPa. Another example is a perfect two-dimensional (2D) waveguide, for example, a shallow sea with a hard bottom and a flat surface. In this case SPL far from the source with respect to the water depth falls as the inverse of distance, and the effect is known as cylindrical spreading. Ocean SPL is controlled by another factor: absorption by

[a]Author to whom correspondence should be addressed.

the boundaries. The effect of boundary absorption on ocean sound and the ocean noise field is roughly analogous to room acoustics. Methods developed for performance-space design in the late 1800s that involve reverberation time and boundary reflection properties can be generally applied to sound transmission and decay problems (Young, 1959). Those studies motivated the development of a simplified model, presented here, capable of capturing the essential physics of ocean sound propagation, while remaining computationally cost effective and allowing separate classes of seafloor-interacting sound to be differentiated.

Here, a model of ambient shipping noise in the ocean is presented. The hypothesis that noise level increases as the absorption coefficient is reduced is tested. The model includes boundary absorption, sound channel ray dynamics (Munk *et al.*, 1995), and four-dimensional variable volume absorption. Using forecasts of oceanic *p*H profiles, noise estimates for years 2050 and 2100 are compared to year 2000 estimates. In general, sound energy loss can be partitioned into intrinsic dissipation (the chemical relaxation absorption process) and dissipation in the seafloor. Expected deep ocean noise level changes at frequencies of 0.1–1 kHz are presented. At 100 Hz, little sound is absorbed, so *p*H-dependent absorption effects are muted. At 1000 Hz and above, sound does not propagate far, also minimizing *p*H-dependent absorption effects. In the center of the band there can be sizable effects. Section 2 explains the model and Sec. 3 shows the results. For a distributed set of sources in the North Pacific, the model yields SPL at any location in the deep basin. The effects illustrated by the results are explained together with artifacts from model simplifications.

2. The model and parameters

The model uses ray dynamics in a sound channel to compute SPL at a given location and depth (x_r, y_r, z_r) from a 2D distribution of sources. Source depth is controllable but is fixed at the surface in this implementation. The seafloor is assumed flat, with fixed density of 1200 $\mathrm{kg/m^3}$, and sound speed of 1700 m/s. The sound-speed profile $c(z)$ is uniform throughout the domain, a stiff approximation that we believe yields results correct to first order. The model in this form is written

$$\langle p^2(x_r,y_r,z_r)\rangle = \int\int dxdy W(x,y)\frac{1}{r}\int_0^{\pi/2} d\theta_1 \frac{2\cos\theta_1}{R(\theta_1)\sin\theta(r)} e^{-\beta(\theta_1,x,y)r} V(\theta_B(\theta_1))^{2r/R(\theta_1)}. \quad (1)$$

Starting from the left, the integral is of source density W over surface area element $dxdy$. The next term is cylindrical spreading loss at the source-receiver range $r(x,y)$, with $r^2=(x-x_r)^2+(y-y_r)^2$. The integral that follows is of ray launch angle with respect to a horizontal plane at the source position, with ray launch angles ranging from zero (horizontal toward the receiver) to $\pi/2$ (downward). The next quotient handles deep-water sound channel physics (ray-tube focusing). The $c(z)$ information yields R, the ray double-loop length (Munk *et al.*, 1995), and θ is the ray angle at range r from the source (and thus depth z_r). This term does not have a strong effect on our calculation. The next term is volume absorption, which is computed for each ray and for each source position. The linear effective absorption coefficient $\beta=\ln(10)\alpha/10$, where α has units dB/km. The computation of β is described later. Next, V is the Rayleigh amplitude reflection coefficient at seafloor ray angle θ_B, which is a function of θ_1. It is subunity for rays with supercritical grazing angle at the seafloor with exponent equal to two times the number of reflections. Without the seafloor effects, the model is equivalent to the average decay law in Brekhovskikh and Lysanov (1991).

The amount of sound energy from a source that reaches any given location is controlled by three mechanisms: (1) subunity value of (effective total) seafloor reflection for super critical rays, (2) loss caused by absorption along ray paths with α acting on individual rays, and (3) spreading loss of $1/r$.

In this implementation the sound channel and depth are fixed, allowing the vast simplification of having one set of rays for all source-receiver pairs and all times. The sound-speed profile $c(z)$ is given by the Munk profile $c(z)=c_a[1+\varepsilon(\exp(\eta)-\eta-1)]$ with $\eta=(z-z_a)/B$ (Munk

et al., 1995). Parameters are $\varepsilon = 0.0057$, scale depth $B = 500$ m, minimum $c(z)$ of $c_a = 1490$ m/s at depth $z_a = 1100$ m, surface sound speed of 1540 m/s, and conjugate depth at about 4500 m. For each θ_1 there is one R, one θ_B, and one V, to be used for all paths connecting each $[x, y]$ and $[x_r, y_r]$. These will actually vary in the ocean as will the seafloor depth, but the initial calculation in this letter makes this (essentially narrow latitude-scope) approximation. The output of the model is the incoherent sum of SPL for many rays, so unbiased errors for each ray should contribute only weakly to the result.

Variation of the absorption term in the model is explained here. First, Community Climate System Model (CCSM-3) ocean model output for the appropriate year is used to compute $\alpha(x, y, z, t, f)$ using the formulas in Brewer *et al.* (1995). The CCSM-3 model, described in the next paragraph, provides the required temperature, salinity and *p*H over a three-dimensional (3D) grid. To provide what is needed for the SPL computation, absorption is tabulated for each ray along each source-receiver path. For each path, the ray trajectories are superimposed on an interpolated vertical slice of frequency dependent $\alpha(x, y, z, t, f)$, then the average of α is computed for each ray, enough to compute the correct effective average β to include in $\exp(-\beta r)$ in Eq. (1).

CCSM-3 consists of an upper-ocean ecological module and a full-depth ocean biogeochemistry module, both embedded in a 3D global physical ocean general circulation model (Doney *et al.*, 2009). The biogeochemistry module simulates the distributions and evolution of dissolved inorganic carbon and alkalinity and includes full seawater carbonate system thermodynamics. The model captures the major processes governing the ocean carbon cycle including physical circulation and mixing, air-sea gas exchange, biological formation and respiration of organic carbon, and precipitation and dissolution of calcium carbonate. The simulations used here are from the fully coupled ocean-atmosphere-land version of CCSM-3 forced with fossil fuel and deforestation carbon emissions from observations for the historical period and the IPCC A2 scenario (business as usual, with regional and economic emphases over global and environmental, see Nakicenovic and Swart, 2000) with high CO_2 emissions in the 21st century (Thornton *et al.*, 2009).

Figure 1 shows CCSM-3 *p*H output in the North Pacific for years 2000 and 2050. Reduction over time is evident. Figure 1 also shows slices of α for 1000 Hz. Figure 2(e) shows positions for 111 sources used in the SPL results shown in this paper [$W(x, y)$ can be thought of as a sum of delta functions at these location]. These are intended to mimic ship traffic between East Asian ports and Western North America and the Panama Canal. Additional sources are placed between Hawaii and North America. Figure 2(e) also shows SPL result locations (x_r, y_r), which all lie along a meridional line except for one to the east. At this eastern location numerous North Pacific Acoustic Laboratory (NPAL) experiments have yielded estimates of noise level to allow calibration of our model. For calibration, twenty 5 min records obtained at 500 m depth are used, randomly chosen over a 7 day period in September 2004. After the model is run with a randomly chosen (2.4 dB rms) distribution of source level for the 111 sources (fixed over time), the SPL result is normalized to match the observations at that location, which agree well with *a priori* noise SPL predictions (75 dB at 100 Hz, 50 dB at 500 Hz, and 40 dB at 1 kHz) based on levels of marine ambient noise for usual traffic in a deep ocean (see Committee on Potential Impacts of Ambient Noise in the Ocean on Marine Mammals, 2003). The wide separation between sources, the incoherent summation to form SPL, the simplifications made to the sound channel, and the smooth nature of the α field, mean that each source in the model can act as the sum of many times this number of sources (see Hildebrand (2009) for a discussion of shipping traffic in the North Pacific). This normalization method allows simulation of noise SPL maps under a variety of conditions without knowing the source spectra of many ship classes, or the distribution of ships in each class within the basin.

Figures 2(a) and 2(b) show α in a selected source-receiver slice for two different time periods. Note the reduction over time in the upper 1000 m, in agreement with results of Ilyina *et al.* (2010). Once again, summation of α along rays within slices like this produces effective absorption β. This is plotted in the Fig. 2(c) versus ray launch angle, for each time period.

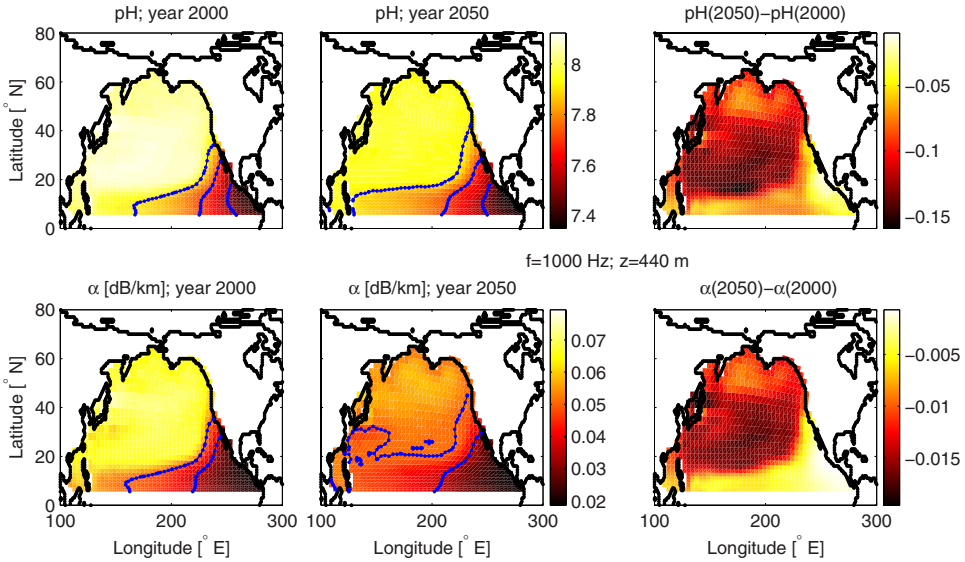

Fig. 1. (Color online) Quantities from the global climate model are plotted for the North Pacific Ocean for the depth layer 440 m. At the top are shown *p*H in the years 2000 (left), 2050 (middle), and the difference between the two years (right). At the bottom are shown absorption coefficients for 1000 Hz, also for the years 2000 (left), 2050 (middle), and the difference between the two years (right). Contours corresponding to *p*H=7.9, 7.7 and 7.5, and corresponding to α=0.035 and 0.05 are shown.

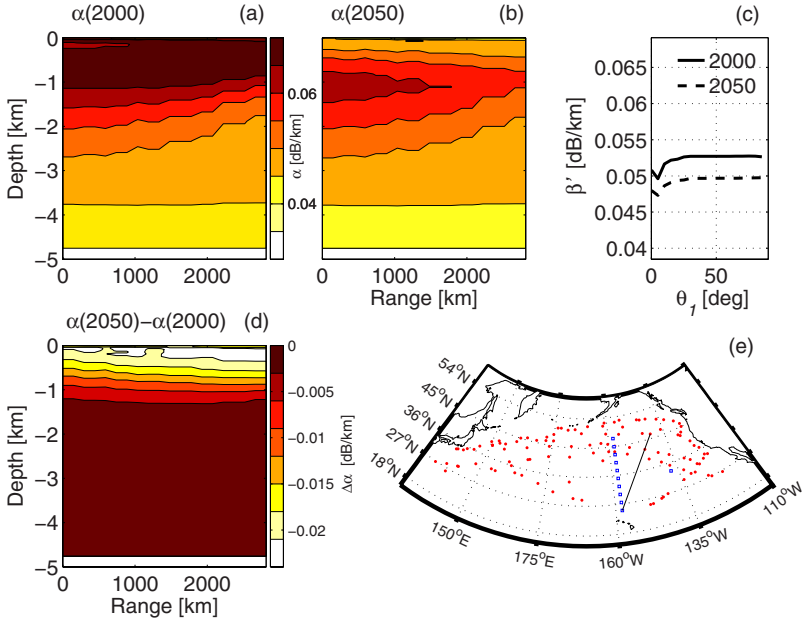

Fig. 2. (Color online) Absorption coefficient α in a source-to-receiver vertical slice is contoured for each of two years, 2000 (a) and 2050 (b) for 1000 Hz. (d) shows the difference between the two. (c) shows, for rays along this transect, the effective absorption coefficient β' (logarithmic version of β) as a function of ray launch angle for each of the years. (e) is a map of the North Pacific Ocean. Locations of noise sources (ships) are plotted with red dots. Noise computation locations [receivers (x_r, y_r)] are shown with blue squares. The line shows the source/receiver path used for (a), (b), and (d).

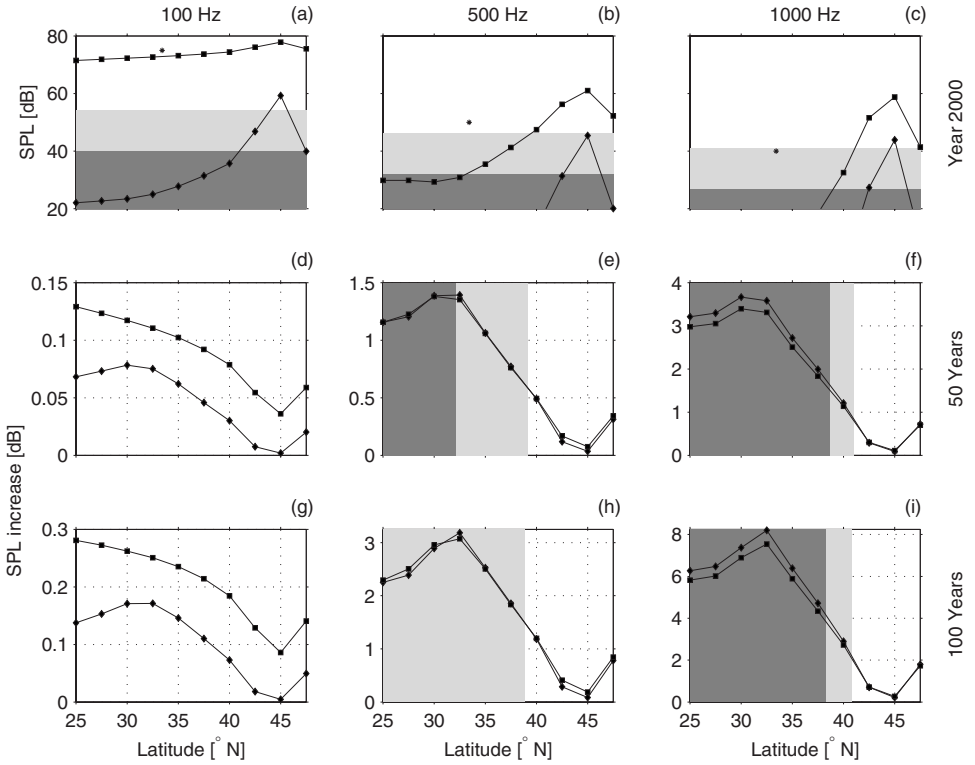

Fig. 3. Results of the shipping noise SPL computations for the meridional section of receivers depicted in Fig. 2(e) are shown. [(a)–(c)] Estimated SPL in year 2000 at 100, 500, and 1000 Hz. [(d)–(f)] Predicted SPL changes over 50 years are plotted for the same frequencies (year 2050 SPL minus year 2000 SPL). [(g)–(i)] SPL changes over 100 years are plotted. In each panel, the total SPL (or the change of the total SPL) is shown with square symbols. The diamond symbols and lower lines show SPL (or change of SPL) associated with steep rays having subunity reflection coefficient. The isolated symbols show SPL at the eastern station that is not on the meridional line. Gray shadings are for two local sound pressure levels; dark for low wave action and no shipping and light for levels slightly below SS2.

3. Results

Results of the SPL calculations at receiver stations [Fig. 2(e)] are plotted in Fig. 3. Receiver depth z_r is 500 m for all stations and computations used α fields for September in the specified year. Note that the stations cross an area with no sources, allowing the effects of source-receiver distance on the result to be examined. At the top [Figs. 3(a)–3(c)], SPL in year 2000 is plotted versus latitude for frequencies of 100, 500, and 1000 Hz. Also plotted are SPL values for a low-energy component of the total arriving energy due to steep rays with subunity reflection coefficient V. Comparison of the curves illustrates that the majority of the total SPL (upper curves) is described by rays that miss the seafloor or reflect at subcritical grazing angle. The low absorption at 100 Hz allows sound to propagate into the area north of Hawaii with no modeled sources. Sound at 500 Hz falls from 60 dB at the northern end of the line to 30 dB at the southern end. Sound at 1000 Hz drops to even lower levels along the line, off the graph. (Note that 1000 Hz level is 40 dB at 33 °N eastern station near sources.) The shaded areas in each panel indicate two levels of noise threshold that are used to judge the significance of the results. The lower level (dark gray) is the so-called lower bound of prevailing noise, 40, 32, and 27 dB (see Committee on Potential Impacts of Ambient Noise in the Ocean on Marine Mammals, 2003) at 100, 500, and 1000 Hz, respectively. This is a guess at what SPL would be in an ocean basin with low wave action and no shipping noise. Levels so low have rarely if ever been observed. The higher levels (light gray) are 14 dB higher at each frequency, chosen to be higher than the low threshold, but somewhat below

the estimate of noise SPL of 60 dB across this band that would result from local surface wave action in sea state 2 (Hildebrand, 2009). Note that the threshold level guides the interpretation of how absorption reduction impacts distant shipping noise.

The center line of Figs. 3(d)–3(f) shows the difference of year 2050 SPL and year 2000 SPL. At 100 Hz [Fig. 3(d)], there is very little change, 0.13 dB maximum (3% increase in energy), indicating that absorption has little effect on the SPL at these locations, for the chosen source distribution. At 500 Hz [Fig. 3(e)] there is a trend toward increased SPL at the southern stations, close to 1 dB (25% increase in energy). Under the sources, at the north, the SPL is essentially unchanged because the dominant arriving sounds have not propagated very far and have not been impacted by absorption. However, sound from the modeled sources arriving at the southern stations is quite low in level, and would probably be not audible compared to the local wind-wave noise. This is indicated by the shaded areas on the left side of the difference figures. The shaded areas mark where SPL is below one or both thresholds in the top panel. Thus, only the SPL at the right in the 500 Hz center panel represent an increase in audible ambient noise. The maximum increase is 0.6 dB (15%). The 1000 Hz results shown in Fig. 3(f) follow the 500 Hz results closely, with the same maximum increase in SPL, although the threshold is crossed at different latitude.

Figures 3(g)–3(i) (lowest row) show the differences of year 2100 and year 2000 SPL, similar to the 2050/2000 differences in the center row. The maximum increase in shipping noise sound is about 1.5 dB for 500 Hz (40% energy increase), and about 2.0 dB for 1000 Hz (58%).

The impact of reduced absorption will only be at great distance, where SPL is low because of geometrical spreading. At some point, the distant noise is very low in the model and will be masked by local noise. However, local noise may increase slightly, and these areas may be noisier even though distant shipping is not responsible. The simulation results can guide us here. Note that the simulations show no increase in ambient sound at 45 °N, where sources are very near the receiver. In this situation, locally generated sound dominates the SPL, and short range r means that absorption $\exp(-\beta r)$ is near unity.

In summary, the very large changes in upper-ocean absorption coefficient predicted to follow carbon dioxide uptake into the ocean from the atmosphere have been modeled to have a small but potentially detectable impact on ocean acoustic noise at 100 to 1000 Hz. Increases of up to 58% in sound energy in 100 years are predicted. These changes may not be audible, however. Increasing the audibility threshold to 55 dB across the frequency band, which could be defended, would place few of the 500 and 1000 Hz results for 2100/2000 and 2050/2000 differences in the audible range, with a maximum effect of roughly 1.0 dB (26% energy increase).

Finally, note that the acoustic model is not comprehensive, and results obtained with a more complete model may vary slightly. This model with fixed ray geometry does not allow down-slope conversion of sound at continental margins, nor conversion of deep-cycling rays to rays trapped closer to the sound channel center in the case of subpolar-generated sound moving southward. The flat bottom approximation for the deep basin causes a slight overestimation of SPL. The effects of this approximation on the differences of SPL in the differing years (differing absorption conditions) are not intuitive and deserve further investigation.

Acknowledgments

This work was supported by the Ocean Acoustics Program at the U.S. Office of Naval Research, Code 321, including an ONR Postdoctoral Fellowship award to the first author.

References and links

Brekhovskikh, L. M., and Lysanov, Yu. P. (**1991**). *Fundamentals of Ocean Acoustics*, 2nd ed. (Springer-Verlag, New York).

Brewer, P. G., Glover, D. M., Goyet, C., and Shafer, D. K. (**1995**). "The *p*H of the North Atlantic Ocean: Improvements to the global model for sound absorption in seawater," J. Geophys. Res. **100**, 8761–8776.

Brewer, P. G., and Hester, K. (**2009**). "Ocean acidification and the increasing transparency of the ocean to low-frequency sound," Oceanogr. **22**, 86–93.

Caldeira, K., and Wickett, M. E. (**2005**). "Ocean model predictions of chemistry changes from carbon dioxide emissions to the atmosphere and ocean," J. Geophys. Res. **110**, C09S04.

Committee on Potential Impacts of Ambient Noise in the Ocean on Marine Mammals (**2003**). *Ocean Noise and Marine Mammals* (National Research Council, Washington, DC).

Doney, S. C., Lima, I., Moore, J. K., Lindsay, K., Behrenfeld, M. J., Westberry, T. K., Mahowald, N., Glover, D. M., and Takahashi, T. (**2009**). "Skill metrics for confronting global upper ocean ecosystem-biogeochemistry models against field and remote sensing data," J. Mar. Syst. **76**, 95–12.

Feely, R. A., Doney, S. C., and Cooley, S. R. (**2009**). "Ocean acidification: Present conditions and future changes in a high-CO_2 world," Oceanogr. **22**, 36–47.

Francois, R. E., and Garrison, G. R. (**1982**). "Sound absorption based on ocean measurements. Part II: Boric acid contribution and equation for total absorption," J. Acoust. Soc. Am. **72**, 1879–1890.

Hildebrand, J. A. (**2009**). "Anthropogenic and natural sources of ambient noise in the ocean," Mar. Ecol.: Prog. Ser. **395**, 5–20.

Ilyina, T., Zeebe, R. E., and Brewer, P. G. (**2010**). "Future ocean increasingly transparent to low-frequency sound owing to carbon dioxide emissions," Nat. Geosci. **3**, 18–22.

Mellen, R. H., and Browning, D. G. (**1977**). "Variability of low-frequency sound absorption in the ocean: pH dependence," J. Acoust. Soc. Am. **61**, 704–706.

Munk, W. H., Worcester, P. F., and Wunsch, C. (**1995**). *Ocean Acoustic Tomography* (Cambridge University Press, New York).

Nakicenovic, N. and Swart, R. (**2000**). *Special Report on Emissions Scenarios: A Special Report of Working Group III of the Intergovernmental Panel on Climate Change*, 1st ed. (Cambridge University Press, Cambridge, UK).

Thornton, P. E., Doney, S. C., Lindsay, K., Moore, J. K., Mahowald, N., Randerson, J. T., Fung, I., Lamarque, J.-F., Feddema, J. J., and Lee, Y.-H. (**2009**). "Carbon-nitrogen interactions regulate climate-carbon cycle feedbacks: results from an atmosphere-ocean general circulation model," Biogeosciences **6**, 2099–2120.

Young, R. W. (**1959**). "Sabine reverberation equation and sound power calculations," J. Acoust. Soc. Am. **31**, 912–921.